Heliyon 10 (2024) e25744

Contents lists available at ScienceDirect

Heliyon

journal homepage: www.cell.com/heliyon

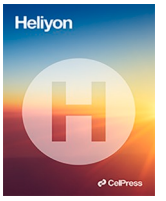

Research article

A novel micro-reactor for hydrogen production from solid $NaBH_4$ hydrolysis in a dual-cycle methodology

Eyal Hayouk [a], Alex Schechter [b], Idit Avrahami [a,*]

[a] Department of Mechanical Engineering & Mechatronics, Ariel University, Ariel, 40700, Israel
[b] Department of Chemical Sciences, Ariel University, Ariel, 40700, Israel

ARTICLE INFO

Keywords:
Hydrogen generator
On demand
Off-grid
Fuel cell
Power pack
Solid sodium borohydride
Mobility
Storage

ABSTRACT

Hydrogen-based Fuel Cells (FCs) hold significant potential as energy conversion technologies. In a previous study, we presented a pump-based hydrogen generator (PHG) that utilizes a catalytic reaction between sodium borohydride ($NaBH_4$) powder and water. The pump circulates the water solution through the powder chamber in a closed-loop reaction. The PHG demonstrated clear advantages over alternative hydrogen sources in terms of both safety and energy density. However, as operating time increases, the solution in the closed-loop PHG becomes saturated, causing the reaction rate to decline. This limitation can be overcome in cases where an external water source is available, such as marine vehicles, drones equipped with water recovery systems from their fuel cells, or systems located near pipelines. In such scenarios, introducing freshwater feeding and product emission offers intriguing possibilities for significantly enhancing the fuel's energy density and extending its effective operation time.

Our current research introduces an innovative concept: a dual-cycle generator (DCG) that effectively overcomes the issue of solution saturation over time. It achieves this by combining solution circulation with freshwater feeding and product emission. Our study employed a DCG prototype to examine various operating modes and to demonstrate the effectiveness of this approach. The DCG achieved a calculated energy density for the fuel of 3868 Wh/kg, with 93% H_2 extraction yield from the powder. Our findings reveal substantial improvements in terms of extended operation duration (81%), increased hydrogen flow rate (36%), enhanced energy density (33%), and improved H_2 yield extraction from the powder (39%). This methodology holds promise for mobile applications or off-grid systems situated in proximity to a water source.

1. Introduction

In the pursuit of effective methods for continuous, efficient, reliable, clean, lightweight, and easily transportable electricity, the necessity emerges to explore substitute approaches to conventional batteries. Even the most advanced lithium-ion batteries can achieve up to 250 Wh/kg [1], and lithium-thionyl chloride batteries mark a limit of 500–600 Wh/kg [2]. Consequently, there has been a growing curiosity in techniques that convert chemical constituents into electrical energy, thereby enabling a continuous and efficient supply of electricity on demand with a notable energy density.

Theoretically, hydrogen (H_2) is regarded as an energy source with a substantially high gravimetric energy density of 33 kWh/kg

* Corresponding author. Dep. of Mechanical Engineering and Mechatronics Ariel University P.O. Box 3, Ariel 44837, Israel.
E-mail address: iditav@ariel.ac.il (I. Avrahami).

https://doi.org/10.1016/j.heliyon.2024.e25744
Received 25 October 2023; Received in revised form 4 January 2024; Accepted 1 February 2024
Available online 8 February 2024

[3]. The efficient conversion of hydrogen into electricity using fuel cells (FCs) can facilitate the continuous supply of electric power at elevated densities. Yet, hydrogen storage presents a critical challenge for energy conversion in FCs, owing to the low density inherent in all forms of hydrogen storage, including cryogenic liquid, high-pressure, and reversible physical storage materials. For portable devices, hydrogen can be stored through high-pressure or low-temperature cylinders. However, due to its low density and safety concerns, the weight percent of hydrogen's gravimetric density in high-pressure gas tanks (~700 bar) remains lower than 5% wt., corresponding to 1650 Wh/kg [4,5]. An alternative procedure for hydrogen storage in cylinders is to produce it by chemical reaction of metal hydride with water (hydrolysis) on-site and "on-demand" with minimal energy investment and relatively high energy density of the fuel (ED_f) [6–8].

This study focuses on Sodium Borohydride ($NaBH_4$, SBH) which is considered relatively available, affordable, lightweight, safe to carry, and has a long shelf life [9,10]. The production of hydrogen involves the catalytic reaction described in Eq. (1) of $NaBH_4$ and a stoichiometric quantity of two molecules of H_2O, theoretically yielding 10.8 wt% of H_2 and the reaction product is Sodium Metaborate ($NaBO_2$) [11].

$$NaBH_4 + 2H_2O \rightarrow NaBO_2 + 4H_2 \tag{1}$$

The product solution has a low environmental footprint and low toxicity [12] and can be either collected and recycled off-site for further hydrogen production or emitted on-site as wastewater (similar to common cleansers, detergents, and adhesives) [11].

In this reaction, H_2O contributes half of the hydrogen content, while the other half is sourced from the $NaBH_4$. For stoichiometric water and SBH reactants, the theoretic gravimetric density of the fuel is very appealing [4,13].

The total weight of the whole system includes the fuel's weight (e.g. powder and water), the reactor, the FC, and the system's components. When extended duration is considered, the fuel's weight becomes dominant and the weight of the system's components becomes secondary (see for example Fig. 7). Therefore, for long operation duration, the relevant parameter is the fuel's energy density (ED_f), which is calculated, according to Eq. (2), from the theoretical obtained energy (E_T), assuming an FC with the efficiency of 60%, and the fuel mass (m_f):

$$ED_f = \frac{E_T}{m_f} = \frac{33_{kWh/kg} m_{H_2} * 60\%}{m_{SBH} + m_{H_2O}} = \frac{20_{kWh/kg} * m_{SBH}(4M_{H_2}/M_{SBH})}{m_{SBH} + m_{SBH}(2M_{H_2O}/M_{SBH})} = 2145_{Wh/kg} \tag{2}$$

where m_{H2} and M_{H2}, m_{H2O} and M_{H2O}, and m_{SBH} and M_{SBH}, are the molar and gravimetric mass of the H_2, water, and SBH, correspondingly.

However, since the reaction requires that the reactants be in a solution form, some access water ($x > n$) is required, according to Eq. (3).

$$NaBH_4 + (2+x)H_2O \rightarrow NaBO_2 nH_2O + 4H_2 + (x - n)H_2O \tag{3}$$

where $n = 4$ is the hydration water trapped by $NaBO_2$ molecules [14,15].

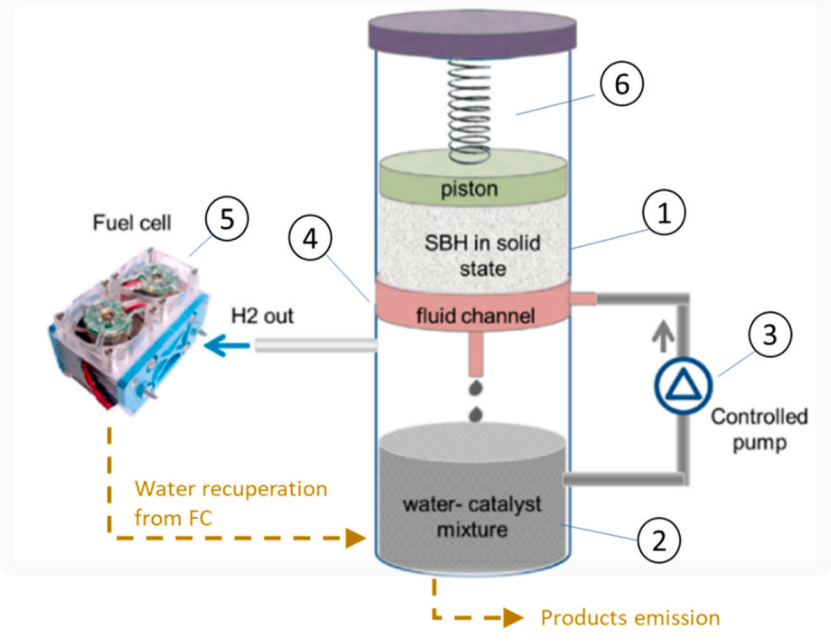

Fig. 1. A schematic description of the pump-based on-demand H_2 generator (adjusted with permission from (Zakhvatkin, Zolotih et al., 2021)). Dashed yellow lines represent the suggested additional components of product emission and recuperated water feeding during generator operation.

Despite its potential, this reaction faces several challenges. The first is linked to the low solubility of $NaBH_4$ in water, necessitating a relatively large excess of water to facilitate the reaction [16,17], thus limiting the energy density of the fuel (SBH solution) up to $ED_f =$ 900 Wh/kg [18–21]. Instead of pre-mixed SBH solutions which require stabilizers and a significant amount of access water, the use of SBH in a powder form allows for much lower water access [15]. In this case, the theoretical energy density with the minimal water for product solubility (x = 4.5) is $ED_f = 1500–1760$ Wh/kg (depending on reaction temperatures). However, the use of powder faces many challenges, involving mixing, heat management, powder gumming, and product crystallization, and therefore the actual reported ED_f in powder-to-water generators is lower ($ED_f = 1400$ Wh/kg) [22,23].

In previous studies conducted in our lab, a novel concept of a pump-based hydrogen generator (PHG) was developed based on well-controlled dosing of SBH solution on-demand [24]. In the PHG, only a thin layer of the solid SBH powder comes into contact with water through an open spiral channel delivering controlled doses of SBH as the water flows toward the reaction chamber. This concept has proven to overcome the numerous technical drawbacks associated with the powder-to-water generator. It allows for a simple, safe, lightweight, and on-demand prolonged operation, featuring a spontaneous process that allows multiple stops and restarts, with a measured energy density of the fuel of $ED_f = 1500$ Wh/kg.

The main structure of the PHG comprises two primary chambers (see Fig. 1): an upper chamber (1) filled with SBH powder in a solid state and a lower reaction chamber (2) containing a water solution and catalyst mixture. A pump (3) circulates the solution from the reaction chamber through an open spiral channel (4) placed at the bottom of the solids chamber, where the solution is in contact with the powder. The solution flowing in the channel becomes saturated with SBH and drips down into the reaction chamber, where the SBH solution interacts with the catalytic particles initiating the reaction. The released hydrogen then flows through an outlet towards the FC (5). To ensure effective contact between the powder and the flowing solution in the channel, the SBH powder is pushed downwards by a piston-spring mechanism (6).

Another development by our group (Zakhvatkin, Schechter et al., 2021) (Zakhvatkin et al., 2022), facilitated a water recovery system (WRS) that recuperates water from the FC's exhaust vapor (e.g. for areal applications). This vapor is collected and condensed into water that can be utilized in the reaction process, thus reducing the weight of the carried water. Thus, the energy density of the fuel (ED_f) may be further increased up to 1800 Wh/kg.

Furthermore, when product emission is also employed, only a small amount of water needs to be maintained in the generator even during prolonged operations. This is due to the consistent replacement and dilution of the high-concentration solution (containing products) by the incoming water feed from the recuperation system. As a result, the constant weight of water in the generator can be

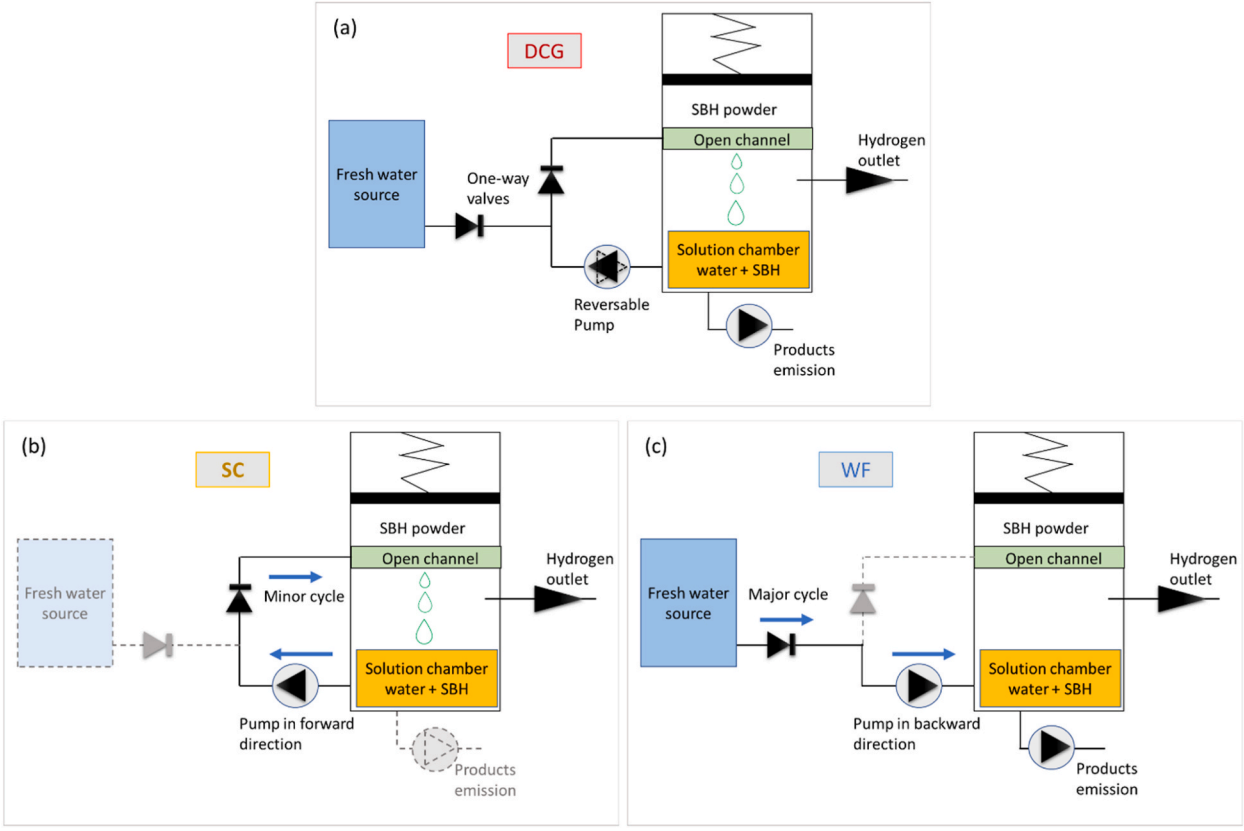

Fig. 2. A schematic description of the dual-cycle generator (DCG); a) the DCG components, including the two-way valves, the reversible pump, and product emission; b) the minor cycle of solution circulation (SC); c) the major cycle with water feeding (WF) and product emission.

considered as a part of the initial weight of the generator. Consequently, the weight of the fuel required for operation encompasses solely the weight of the SBH powder.

If only the weight of the SBH powder in the fuel's weight ($m_f = m_{SBH}$) is considered, the theoretical energy density of the fuel for long operation durations may reach up to $ED_f = 33_{kWh/kg} \cdot 0.6(4M_{H_2}/M_{SBH}) = 4190_{Wh/kg}$. The weight of the water is then added to the weight of the system's components (including the generator and the FC). This method may find applicability for mobile applications with WRS or any off-grid systems located near a water source (such as marine vehicles, pipeline infrastructures, agriculture, etc.).

In the current study, we examine the option of combining freshwater feeding and product emission within the PHG during its operation (indicated by dashed yellow lines in Fig. 1) to extend the operation duration and enhance the fuel's energy density. To realize this, we have designed a novel generator concept that allows water from an external source to be fed into the generator during operation. Furthermore, this new model incorporates a component that enables product emission prior to each water feeding cycle, ensuring a consistent fluid level within the generator at all times.

The novel concept suggested here is a dual-cycle generator (DCG) based on the basic PHG (Fig. 1), with additional components that include two one-way valves and a reversible pump that can operate in two directions (Fig. 2a). The concept includes two main operation cycles: the first is a 'minor cycle' (Fig. 2b), in which the pump operates in the forward direction, performing *Solution Circulation* (SC), similar to the original generator (Fig. 1). The second is a 'major cycle', (Fig. 2c), in which the pump is operating in the opposite direction and performs *water feeding* (WF) from an external source (e.g., water recuperated from the FC) and product emission during the generator operation. The combination of SC and WF within the DCG has the potential to enhance the management of solution concentration and temperature during operation, thereby improving the fuel's energy density and hydrogen yield from the SBH and extending the effective operational durations. Furthermore, the suggested generator offers adaptable modes of operation, with diverse combinations of minor and major cycles.

This manuscript presents an experimental apparatus in which the feasibility of the DCG is demonstrated, and the impact of operation parameters on the fuel's energy density and process efficiency is explored.

2. Methods and materials

2.1. The experimental apparatus

The experimental setup is shown in Fig. 3. Fig. 3a shows the system's components and Fig. 3b shows the assembled system. The generator is composed of two plastic chambers (400 ml each). The SBH chamber contains a spiral channel and a piston spring mechanism (both 3D-printed). Both chambers are placed inside a sealed casing with a hydrogen outlet at the top and tubes connected at the bottom for fluids management and product emission. The tubes are connected to two peristaltic pumps (12V Peristaltic Dosing Pump, Kamoer) through one-way valves. One is the reversible pump, and the other is for the emission of saturated solution with products.

The control system includes a pressure sensor (MPX5100DP, NXP), a k-type thermocouple, and a hydrogen flow meter (ALIMS-2SLPM-D[H_2], Alicat Scientific). Hydrogen pressure in the system did not exceed 0.7 bar.

The reversible pump was set to operate at flow rates of 50 ml/min every 4–5 min for 4–5 s, either in a forward direction (SC) or backward direction (WF), depending on the examined case's protocol. The product emission pump operated before each WF stage to

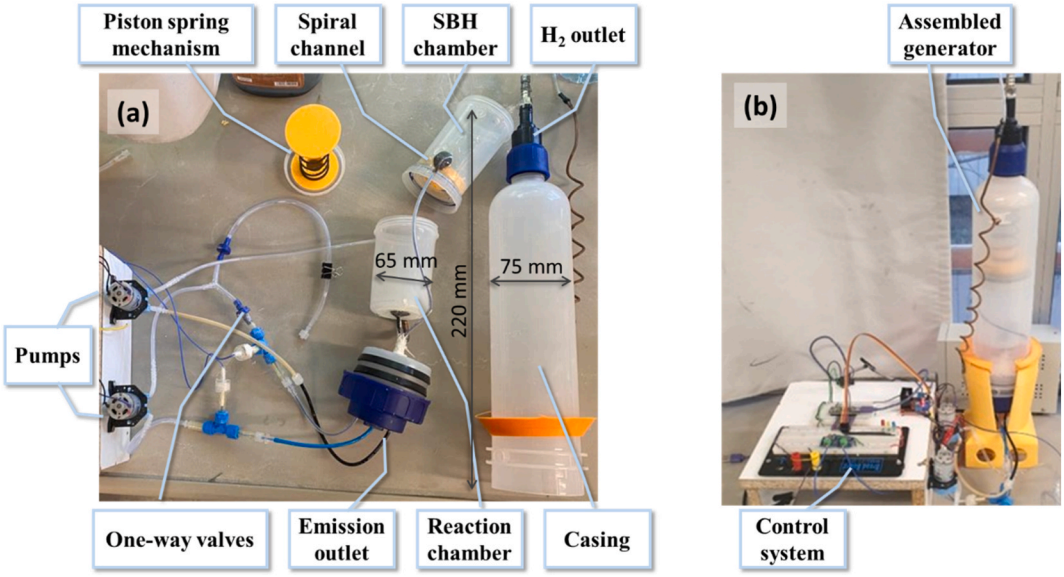

Fig. 3. The experimental system, a) system's assembly, and b) system's components.

maintain a constant solution volume of 200 ml in the reaction chamber.

A series of five experiments were conducted (see Table 1), with different combinations of SC and WF cycles. In each case, the reaction chamber was initially filled with 200 ml of water and 0.02 g of suspended Ruthenium anchored on carbon nanoparticles (Strem Chemicals 44–4050), and the SBH chamber was filled with 10 g of granulated SBH powder (Acros Organics, CAS:16940-66-2, 98% granules with 3 mm average diameter). The fresh-water container was kept at a constant temperature as described in Table 1.

2.2. Performance parameters

The generator efficiency and performance for each case are examined using five main performance parameters: the average flow rate (Q_{avg}), the effective operation duration (t_{oper}), the total volume of water used (V_{H_2O}), H_2 yield from powder (α_{yield}), and Fuel's Energy Density (ED_f).

The average flow rate (Q_{avg}) is calculated using Eq. (4):

$$Q_{avg} = \frac{V_{H_2}}{T} = \frac{1}{T}\int_0^T Q_{H_2}(t)dt \tag{4}$$

where V_{H_2} is the volume of extracted hydrogen, $Q_{H_2}(t)$ is the instantaneous hydrogen flow rate as measured by the flow meter and T is the total duration of the experiment ($T = 105$ min).

The effective operation duration (t_{oper}) is defined in Eq. (5) as the total time during which the hydrogen flow rate remained above the operational flow rate of 180 ml/min, necessary to generate 16 Watts in a commercial FC [25]:

$$t_{oper} = t_{Q>180\frac{ml}{min}} \tag{5}$$

The total volume of water used (V_{H_2O}) is the sum of the initial volume ($V_{init} = 200$ ml) and total feeding volume in each case (Eq. (6)).

$$V_{H_2O} = V_{init} + V_{feed} \tag{6}$$

H_2 yield from powder (α_{yield}) is calculated (Eq. (7)) as the fraction between the total extracted hydrogen volume and the theoretical stoichiometric quantity that could have been obtained (referred to as V_{stoch}).

$$\alpha_{yield} = \frac{V_{H_2}}{V_{stoch}} \bullet 100\% \tag{7}$$

where V_{stoch} is calculated (Eq. (8)) from the SBH mass ($m_{SBH} = 10$ g), hydrogen molar mass ($M_{H_2} = 2.016\frac{gr}{mole}$), SBH molar mass ($M_{SBH} = 37.83\frac{gr}{mole}$), and hydrogen density at STP condition ($\rho_{H_2} = 0.0898\frac{gr}{liter}$).

$$V_{stoch} = \frac{4 \bullet M_{H_2} \bullet m_{SBH}}{\rho_{H_2} \bullet M_{SBH}} \tag{8}$$

Since product emission ensures that the weight of the system (including the water) is constant, the fuel's energy density (ED_f) is calculated (Eq. (9)) as the ratio between the theoretically obtained energy from the hydrogen (assuming 60% FC efficiency) and the weight of the powder:

$$ED_f = \frac{V_{H_2} \bullet \rho_{H_2} \bullet 33.6\left[\frac{kWh}{kg}\right] \bullet 60\% - E_{inv}}{m_{SBH}} \tag{9}$$

where E_{inv} is the total energy invested in the pumps and in heating of the feed water (Eq. (10)),

$$E_{inv} = 1.163 \bullet \left(T_{feed} - T_{inf}\right) \bullet V_{feed} \bullet \rho_{H_2O} + E_{pumps} \tag{10}$$

where $T_{inf} = 25°C$ is room temperature, T_{feed} is the feed temperature (detailed in Table 1), $\rho_{H_2O} = 1000\frac{gr}{liter}$ is water density, and E_{pumps} is the total electrical energy (approximated 0.1 to 0.25 Wh) invested in the pumps, calculated from the pumps' power (5 Watt) and their total operation durations: $E_{pumps} = (5\ Watt)\ x\ (n_1 * t_{pump} + n_2 * t_{pump})$, when n_1 and n_2 are the numbers of operations for each

Table 1
The five studied cases.

Case name	Specifications	Feeding temperature
OSC	Only solution circulations - as a closed-loop reactor	–
1SC	1 SC following each water feeding – as an open-bed reactor	45±2 °C
2SC	2 SC between each WF cycle – DCG	45±2 °C
4SC	4 SC between each WF cycle – DCG	45±2 °C
4SCHT	4 SC between each WF cycle – DCG	55±2 °C

pump and $t_{pump} = 5$ s.

3. Results

The results of the obtained hydrogen flow rate as a function of time for the first three cases (OSC, 1SC, and 4SC) are shown in Fig. 4. The purple dashed line at a flow rate of 180 ml/min represents a threshold of the minimum operative flow rate for the Fuel Cell.

At the beginning, rapid high flow rates (of about 550–600 ml/min) are observed in all the cases, followed by moderate declines due to solution concentration and powder runout. The local spikes in the flow rate signify the occurrences of circulation (marked by dots) or feeding (marked by stars) events. It is clearly shown that the OSC case reaches the 180 ml/min threshold sooner (after 32 ± 1 min) than the 1SC case (after 42 ± 1 min), and the 4SC case has the longest operation duration (*t*oper) before declining below the threshold (after 49 ± 1 min). This implies that the DCG method enables longer operation time or higher average flow rates for the same amount of powder.

Fig. 5 shows the hydrogen flow rate for the three DCG cases (with 4 SC, 2 SC, and 4 SC at high feeding temperature, 4SCHT). Here again, high flow rates (390–680 ml/min) are followed by gradual declines, resulting in operation durations (*t*oper) of 47–58 min. Notably, the longest duration is achieved by the 2SC case (green curve). This suggests that in the current apparatus, feeding every two SC cycles in the tested method allows longer operation than feeding every 4 SC. It is also shown that when the inlet feeding is heated to 55±2OC (black curve), the H2 flow rate initially reaches higher values (680 ± 0.2 ml/min). However, the subsequent decline is more rapid. Consequently, the operating duration for the 4SCHT case is only 47 ± 1 min, marking the shortest duration among the examined DCG cases. The results are in line with the expected higher reaction rate at higher temperatures, leading to faster consumption of the added NaBH4.

The results of the analysis from the five separate experiments, along with their corresponding performance parameters calculated using equations (4)–(10), are summarized in Table 2 and visualized through bar graphs in Fig. 6.

The operation duration (*toper*) varies between 32 and 58 min (Fig. 6a), while the average flow rate (*Qavg*, based on $T = 105$ min) varies from 150 to 205 ml/min (Fig. 6b). The fuel energy density of the powder (based on Eq. (9) spans from 2900 to 3868 Wh/kg (Fig. 6c), the H2 yield from powder ranges between 67 and 93% (Fig. 6d), and the volume of water used ranges between 200 and 400 ml (Fig. 6e).

Among the five cases, the OSC case (representing the closed-loop reactor) exhibits the lowest performance parameters. Comparatively, the 1SC case (representing the open-bed reactor) demonstrates slightly improved performance, albeit demanding twice the amount of water supply for feeding (400 ml vs. 200 ml). In contrast, the three DCG cases necessitate a lower volume of feeding water than the 1SC, while presenting higher parameters of flow rate, energy density, H_2 yield, and operation duration.

4. Discussion

In this paper, we suggest a novel approach for a combined hydrogen generator. To illustrate the benefits of the suggested concept, a prototype of the generator was constructed and evaluated under five different typical operational scenarios, each depicting varying combinations of *solution circulation* and *water feeding* in the generator. For each case, we examined four key performance parameters: effective operational time (defined as the duration during which the flow rate exceeded the 180 ml/min required by the FC), H2 yield from the powder (expressed as a percentage of the theoretical H2 volume), H2 flow rate, and the energy density of the fuel (calculated based solely on the SBH mass, and incorporating power expended for heating and pumping).

Fig. 4 depicts three mixing concepts employed within the reaction generator: a closed loop reactor without feeding or product emission (indicated by the yellow curve, OSC), an open bed reactor (indicated by the blue curve, 1SC), and a combined reactor featuring periods of solution circulation and dilution (denoted by the red curve, 4SC). It is well shown that even in scenarios involving an unlimited source of fresh water, the combined approach of solution circulation and solution dilution (DCG) is preferred over the open-bed process (1SC). This preference is attributed to the DCG method yielding enhanced hydrogen extraction from the powder,

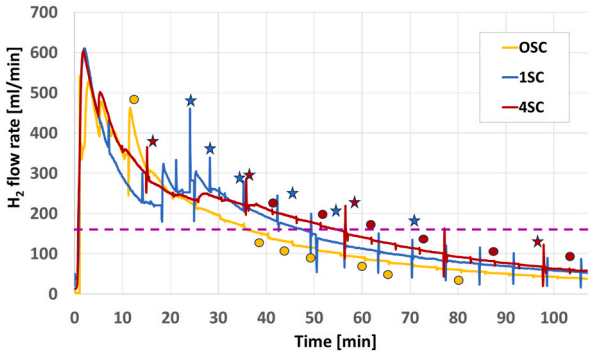

Fig. 4. Hydrogen flow rate as a function of time for the cases OSC, 1SC, and 4SC. Local spikes indicate events of circulation (dots) or feeding (stars). The purple dashed line indicates an operation threshold of 180 ml/min.

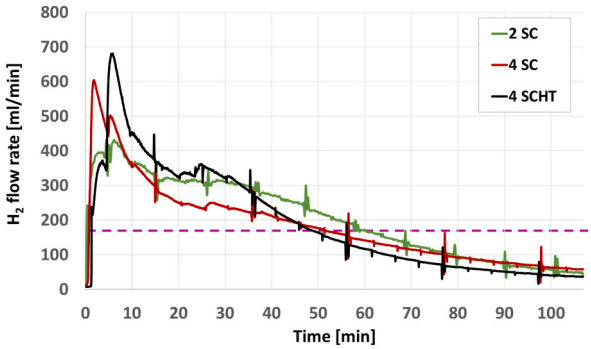

Fig. 5. Hydrogen production flow rate as a function of time for the three DCG cases (4SC, 4SCHT, and 2SC). The purple dashed line indicates an operation threshold of 180 ml/min.

Table 2
Detailed performance parameters of the five cases.

Case Name	Specifications	t_{oper} [min]	Q_{avg} [ml/min]	α_{yield}	ED_f [Wh/kg]	V_{H_2O} [ml]
OSC	Closed-loop reactor	32 ± 1	150 ± 0.1	67 ± 2 %	2900 ± 20	200 ± 5
1SC	Open-bed reactor	42 ± 1	167 ± 0.1	76 ± 2%	2956 ± 20	400 ± 5
2SC	DCG with 2 SC/1WF	58 ± 1	205 ± 0.1	93 ± 2%	3868 ± 20	275 ± 5
4SC	DCG with 4 SC/1WF	49 ± 1	184 ± 0.1	83 ± 2%	3507 ± 20	250 ± 5
4SCHT	DCG with 4 SC/1WF, heated	47 ± 1	191 ± 0.1	86 ± 2%	3606 ± 20	250 ± 5
	Improvement (2SC vs. OSC)	81 ± 9%	36.7 ± 0.2%	39 ± 7%	33 ± 7%	−38 ± 5%
	Improvement (2SC vs. 1SC)	38 ± 5%	22.8 ± 0.2%	22 ± 6%	31 ± 7%	+31 ± 5%

Among the DCG cases, the 2SC obtained the best performances with *t*oper = 58 ± 1 min, *Q*avg = 205 ± 0.1 ml/min, *α*yield = 93 ± 2%, and *ED*f = 3858 ± 20 Wh/kg. The 2SC case has improved operation time by 82% over the OSC case and improved *Q*avg, *α*yield, and *ED*f by 37%, 39%, and 33%, respectively, at the expense of an increased required water volume of 38%.

higher average flow rates, and prolonged operation durations, consequently resulting in higher fuel energy density while utilizing only a quarter of the feeding water (50 ml vs. 200 ml).

Furthermore, by altering the combination of SC and WF in the DCG from 4SC to 2SC, the performance experiences further enhancement across all parameters. The longest operation duration is achieved in the 2SC operation, extending by 82% compared to the OSC case.

If a buffer is used downstream of the hydrogen outlet, a more uniform flow rate may be achieved with the average value of each case (see Table 2). In this scenario, the three DCG cases allow for a sufficient flow rate above 180 ml/min for 105 min, while the OSC and 1SC cases reach only 150 and 167 ml/min, respectively.

Overall, this study demonstrates that the DCG method facilitates enhanced hydrogen production and utilization of the powder (up to 93%) using the same initial quantities of water and powder. While slightly more feeding water is required (75 ml vs. 50 ml), this increase is still less than that of the open-bed case, which consumes an additional 200 ml for feeding.

The impact of reaction temperature is another aspect of this study. Heating the fed water (4SCHT) to 55 °C results in a higher reaction rate, subsequently leading to an increase in average flow rate and H_2 yield extraction without compromising operation duration. Moreover, even though the energy invested in the heating is higher compared to the 4SC case (40–50 °C), the obtained energy density of the 4SCHT case is higher for the same amount of water. Feeding water can be heated using a local electrical heater or by harvesting heat from the FC or the emitted solution. This way, the actual ED_f may be further increased.

İskenderoğlu et al. [26] suggested an example of an autonomous pump-based hydrogen generator that uses a closed-loop control for activating the pump when low flow rates are measured. This control method requires an expensive and heavy flowmeter in the system that might affect the energy density of the applicative system. In previous studies [24] we suggested a closed-loop control system based on pressure measurements, which is more simple and light. In the current study, we present a more basic system with a constant period protocol. Additional study needs to be performed to optimize the specific control method, based on the actual application (and its environment).

The study has some limitations; among them are some non-uniform distribution of Ruthenium catalyst particles within the reaction chamber, The potential for negligible hydrogen leakage from tube connections, and the non-uniform distribution of powder in the powder chamber. Using relatively long tubes (for control and measurements) introduces dead volume in the solution during circulation or feeding (~70 ml), potentially causing delays in the mixing process affecting solution temperature, and significantly raising the water volume used in the system. Additionally, some H2 bubbles from the reaction possibly entered the tubes and influenced the solution flow rates.

The experimental system was constructed using off-the-shelf containers and components; therefore, the prototype is heavier than what is ideally possible. In addition, due to technical issues, we used the solution at the bottom of the fluid chamber for sealing. This

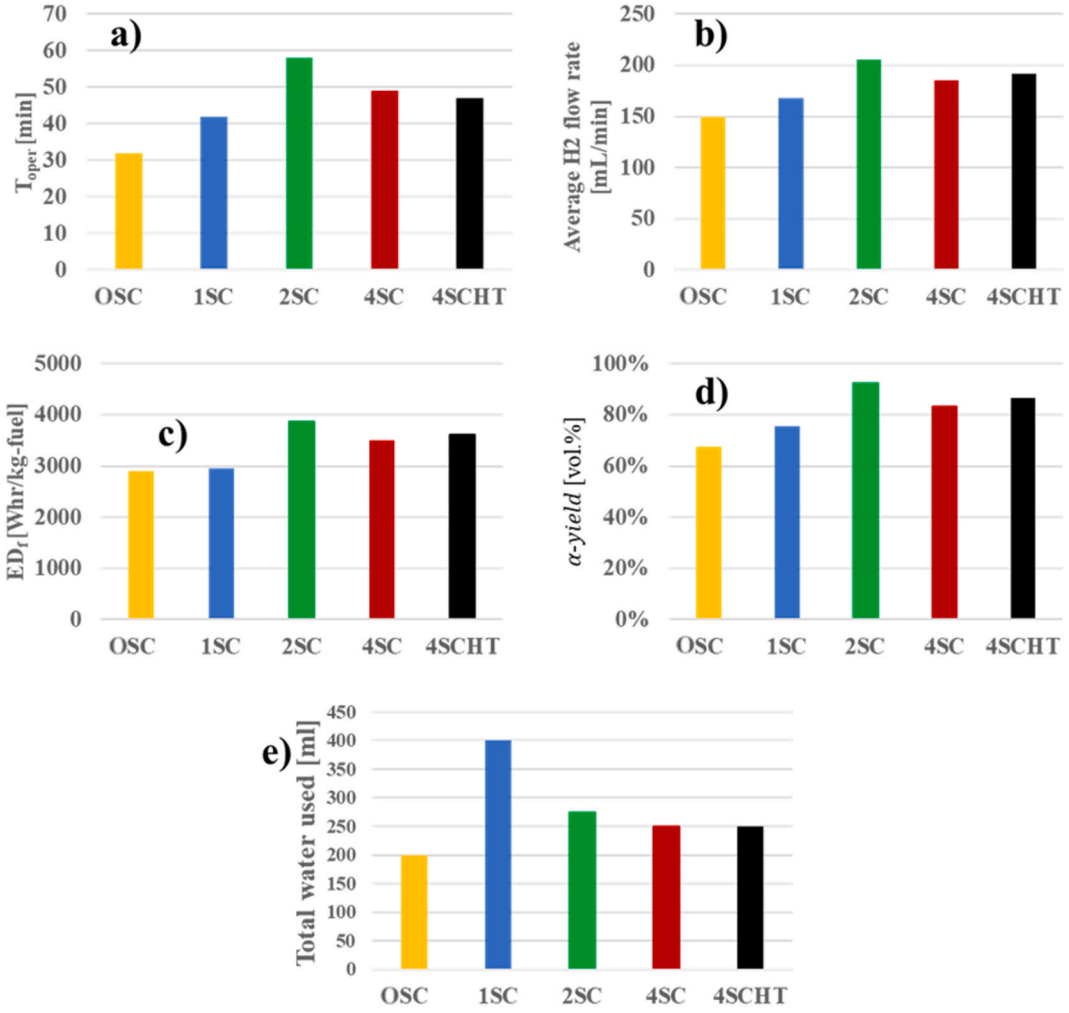

Fig. 6. Calculated performance parameters: a) operation time (t_{oper}); b) Average H_2 flow rate; c) fuel's Energy Density; d) H_2 yield from powder (ayield); and e) Net amount of H_2O used, for the five experiments (OSC, 1SC, 2SC, 4SC, and 4SCHT).

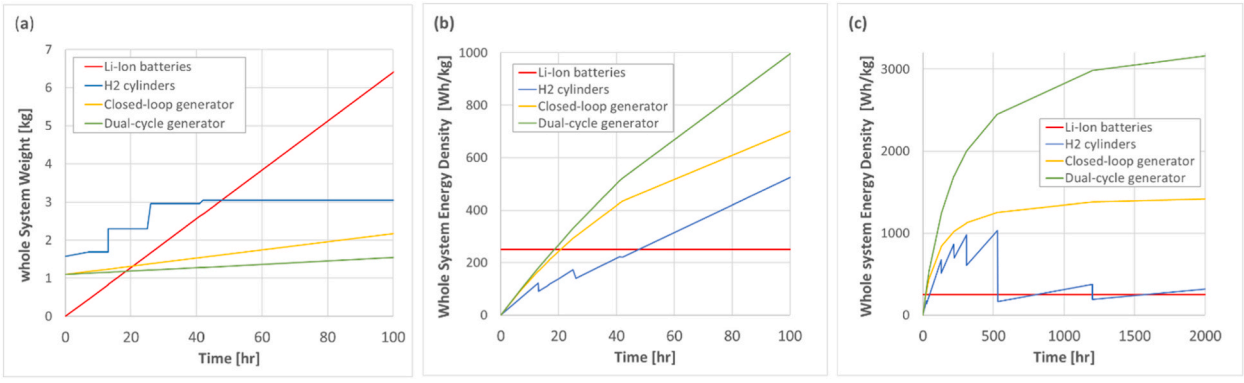

Fig. 7. Comparison of whole system weight (a) and energy density (b,c) for extended-duration operation on 16 W between the currently developed system (DCG) and other alternatives: H_2 cylinders, and a closed-loop generator (OSC).

required almost 100 ml of solution which is much larger than the required from stochiometry of SBH quantity. Altogether, the water access in the pipeline and the fluid chamber reached $x = 40$ (instead of the required x = 5). Thus, the total weight of the generator, including the water (200 ml), the pumps, and the control system, was 0.85 kg. Therefore, the system's energy density does not represent the final application. These limitations might slightly impact the quantitative values for a specific generator configuration; however, they should not impact the impression regarding the proven benefits of the DCG concept, which is well demonstrated by the presented example.

Moreover, when long durations are considered ($toper$>50 h), the only weight accumulated in this system is of the SBH powder, thus, the calculated energy density for long duration is based on the powder alone (Eq. (9)). Fig. 7 simulates and compares the weight of the whole system (a), and the energy density (b) required for a given energy quantity of 16 W across three hydrogen sources: FC derived from H2 cylinders, a closed-loop PHG (OSC), and a DCG. For Li-Ion batteries, we assume an energy density of 250 Wh/kg.

For the H_2 cylinders and the H_2 generators, a 0.3 kg FC with 60% efficiency was assumed. The H2 cylinders, made of seamless aluminum operating at 250–300 bars, have their weight estimated based on data [27] and commercial resources. The PHG consisted of a 0.65 kg generator and 200 ml of water. The estimated fuel weight in the PHG is determined through a simulation based on the experimental results.

It is evident that even with this non-optimized PHG design, the DCG outperforms the other presented alternatives for extended operation durations exceeding 20 h, and for extended durations (of over 500 h) the energy density of the whole system exceeds 2500 Wh/kg. It is important to note that the staircase-like curve in the tank's weight results from the discrete nature of commercial H_2 cylinders selected for this comparison [5,27].

Note that the prototype used here is not optimally designed. With improved design, the expacted system's total weight is 0.5 kg (including a 0.3 kg fuel cell, which is also required in other systems utilizing H2 cylinders). For such a case, the weight of the whole system with PHG is lower than that of a batteries powered system after 7 h of operation.

Future work will aim to improve the suggested DCG and generalize the method for various generator configurations, scales, and operation conditions through the use of an analytical model.This model will delve into the complex dynamics between concentration and temperature in the catalytic reaction and assist in delineating the effect of the different parameters on the DCG outcomes and the prediction and improvement of the generator's performance using a parametric investigation.

Further study will discuss the power pack as a whole system, including the hybrid configuration of the generator, the fuel cell, the water recuperation system, and a battery, connected to a power device demonstrator.The suggested DCG may provide a unique, compact, safe, and simple solution for on-demand hydrogen generation, serving a wide range of off-grid power applications.

5. Conclusions

We successfully demonstrated the concept of integrating solution circulation and freshwater feeding during H_2 dual-cycle generator (DCG) operation. The proposed DCG offers several advantages, including significantly longer operation durations (an 82% increase compared to a closed-loop generator), higher H_2 yield extracted from the powder (referred to as α_{yield}), greater fuel energy density (ED_f), and an enhanced average H_2 flow rate.

Even when an unlimited water source is available, the combination of solution circulation and freshwater feeding in the DCG outperforms the open bed generator. Furthermore, elevating the feeding temperatures has the potential to further boost the reaction rate, average flow rate, and hydrogen extraction yield without compromising the energy density for the same given amount of water and powder. Fine-tuning the specific combination of circulation and feeding cycles may lead to further performance improvements and necessitates a comprehensive parametric investigation.

Funding

This study is supported by a grant from the Israeli Ministry of Energy (grant number: 219-11-136). Eyal Hayouk was partly supported by "DROR" scholarship provided by Ariel University.

Institutional review board statement

This study did not require ethical approval.

Data availability statement

Data is contained within the article or supplementary material.

CRediT authorship contribution statement

Eyal Hayouk: Writing – review & editing, Writing – original draft, Validation, Resources, Methodology, Investigation, Data curation, Conceptualization. **Alex Schechter:** Writing – review & editing, Writing – original draft, Supervision, Resources, Project administration, Investigation, Funding acquisition. **Idit Avrahami:** Writing – review & editing, Writing – original draft, Supervision, Resources, Project administration, Methodology, Funding acquisition, Conceptualization.

Declaration of competing interest

The authors declare the following financial interests/personal relationships which may be considered as potential competing interests:

Idit *Avrahami and Alex Schechter report* financial support *was provided by Israel Ministry* of Energy. Idit *Avrahami and Alex Schechter* report a relationship with NugenX clean energy LTD. that includes: board membership and equity or stocks. Idit Avrahami and Alex Schechter have patent #U.S. patent No. 20210371276: Alex Schechter and Idit Avrahami, "System, device and method for hydrogen production ". Eyal Hayouk declare that he has no known competing financial interests or personal relationships that could have appeared to influence the work reported in this paper.

Acknowledgments

We would like to thank Dr Lev Zakhvatkin, Mr. Ofer Dolitzky, Mr. Georgy Katz, Mr. Ofir Boaron, and Mr. Moshe Deree for their assistance.

References

[1] H. Li, Practical evaluation of Li-ion batteries, Joule 3 (4) (2019) 911–914.
[2] D. Wang, et al., The effects of pore size on electrical performance in lithium-thionyl chloride batteries, Frontiers in Materials 6 (2019) 245.
[3] H. Buchner, The hydrogen/hydride energy concept, International Journal of Hydrogen Energy 3 (4) (1978) 385–406.
[4] D. Santos, C. Sequeira, Sodium borohydride as a fuel for the future, Renewable and Sustainable Energy Reviews 15 (8) (2011) 3980–4001.
[5] R. Ahluwalia, et al., System analysis of physical and materials-based hydrogen storage, in: 2019 Annual Progress Report to the DOE Hydrogen and Fuel Cells Program, 2019. Available at: https://www.hydrogen.energy.gov/pdfs/progress19/h2f_st001_ahluwalia_2019.pdf. (Accessed 7 July 2020).
[6] R. Retnamma, A.Q. Novais, C. Rangel, Kinetics of hydrolysis of sodium borohydride for hydrogen production in fuel cell applications: a review, International Journal of Hydrogen Energy 36 (16) (2011) 9772–9790.
[7] P. Gislon, G. Monteleone, P. Prosini, Hydrogen production from solid sodium borohydride, international journal of hydrogen energy 34 (2) (2009) 929–937.
[8] H.N. Abdelhamid, A review on hydrogen generation from the hydrolysis of sodium borohydride, international journal of hydrogen energy 46 (1) (2021) 726–765.
[9] J. Mao, D.H. Gregory, Recent advances in the use of sodium borohydride as a solid state hydrogen store, Energies 8 (1) (2015) 430–453.
[10] B.H. Liu, Z.P. Li, S. Suda, Solid sodium borohydride as a hydrogen source for fuel cells, Journal of Alloys and Compounds 468 (1–2) (2009) 493–498.
[11] W. Chen, et al., Hydrolysis and regeneration of sodium borohydride (NaBH4)–A combination of hydrogen production and storage, Journal of Power Sources 359 (2017) 400–407.
[12] S.A. Hubbard, Comparative toxicology of borates, Biological Trace Element Research 66 (1998) 343–357.
[13] I. Merino-Jiménez, et al., Developments in direct borohydride fuel cells and remaining challenges, Journal of Power Sources 219 (2012) 339–357.
[14] E.Y. Marrero-Alfonso, et al., Hydrolysis of sodium borohydride with steam, International Journal of Hydrogen Energy 32 (18) (2007) 4717–4722.
[15] J. Yao, et al., Application-oriented hydrolysis reaction system of solid-state hydrogen storage materials for high energy density target: a review, Journal of energy chemistry (2022).
[16] U. Demirci, O. Akdim, P. Miele, Ten-year efforts and a no-go recommendation for sodium borohydride for on-board automotive hydrogen storage, International Journal of Hydrogen Energy 34 (6) (2009) 2638–2645.
[17] U.B. Demirci, Exploring the technological maturity of hydrogen production by hydrolysis of sodium borohydride, International Journal of Hydrogen Energy (2023).
[18] S.C. Amendola, et al., An ultrasafe hydrogen generator: aqueous, alkaline borohydride solutions and Ru catalyst, Journal of Power Sources 85 (2) (2000) 186–189.
[19] J. Kim, T. Kim, Compact PEM fuel cell system combined with all-in-one hydrogen generator using chemical hydride as a hydrogen source, Applied energy 160 (2015) 945–953.
[20] E.S. Jung, et al., Fuel cell system with sodium borohydride hydrogen generator for small unmanned aerial vehicles, International Journal of Green Energy 15 (6) (2018) 385–392.
[21] T.H. Oh, et al., Sodium borohydride hydrogen generator using Co–P/Ni foam catalysts for 200 W proton exchange membrane fuel cell system, Energy 90 (2015) 1163–1170.
[22] I. Avrahami, et al., Hydrogen production on-demand by hydride salt and water two-phase generator, International Journal of Hydrogen Energy (2020).
[23] Y. Nagar, et al., Modeling the mechanical behavior of sodium borohydride (NaBH 4) powder, Materials & Design 108 (2016) 240–249.
[24] L. Zakhvatkin, et al., Hydrogen production on demand by a pump controlled hydrolysis of granulated sodium borohydride, Energy & Fuels 35 (14) (2021) 11507–11514.
[25] Fuel_Cell_Earth, H-20 Fuel Cell Stack User Manual, 2022. https://www.fuelcellearth.com/wp-content/uploads/2018/10/horizon-pem-fuel-cell-h-20-manual.pdf.
[26] F.C. İskenderoğlu, et al., An autonomous hydrogen production system design based on the solid chemical hydride, European Mechanical Science 6 (4) (2022) 213–220.
[27] C.G. Association, Compressed gas cylinders, regulators, and valves, in: Handbook of Compressed Gases, Springer, 1999, pp. 69–80.